



30

31 **Contents**

32 Table S1. The best docking pose scores and the RMSD values of the docking structures  
33 relative to the crystallographic structures ..... 3

34 Figure S1. The root-mean-square deviations (RMSD) of the ligands in the 20 complex  
35 systems. .... 5

36 Figure S2. The individual energy term contributions of key residues to the binding free  
37 energies of (A) NS5B<sup>GT1a</sup>/HCV-796, (B) NS5B<sup>GT1b</sup>/HCV-796, (C) NS5B<sup>GT2a</sup>/HCV-796, and  
38 (D) NS5B<sup>GT2b</sup>/HCV-796 systems. .... 6

39 Figure S3. The energetic difference ( $\Delta\Delta G = \Delta G_{NS5B^{GT1b/GT2a/GT2b}/inhibitor} -$   
40  $\Delta G_{NS5B^{GT1a}/inhibitor}$ ) spectra of the corresponding key residues between the NS5B<sup>GT1a</sup>  
41 system and the NS5B<sup>GT1b</sup> system, NS5B<sup>GT2a</sup> system, or NS5B<sup>GT2b</sup> system. (A) NS5B/HCV-  
42 796; (B) NS5B/BMS-929075; (C) NS5B/MK-8876; (D) NS5B/compound 2; (E)  
43 NS5B/compound 9B..... 7

44 Figure S4. Distances between HCV-796 and residues during the last 20 ns MD trajectories... 8

45 Figure S5. The energetic difference spectra between the NS5B<sup>GT1a</sup>/HCV-796 system and the  
46 NS5B<sup>GT1a</sup>/BMS-929075, NS5B<sup>GT1a</sup>/MK-8876, NS5B<sup>GT1a</sup>/compound 2 or NS5B<sup>GT1a</sup>/compound  
47 9B system ( $\Delta\Delta G = \Delta G_{NS5B^{GT1a}/(BMS-929075/MK-8876/compound\ 2/compound\ 9B)} -$   
48  $\Delta G_{NS5B^{GT1a}/HCV-796}$ )..... 9

49 Figure S6. The binding modes of (A) NS5B<sup>GT1a</sup>/HCV-796 versus NS5B<sup>GT1a</sup>/BMS-929075, (B)  
50 NS5B<sup>GT1a</sup>/HCV-796 versus NS5B<sup>GT1a</sup>/MK-8876, (C) NS5B<sup>GT1a</sup>/HCV-796 versus  
51 NS5B<sup>GT1a</sup>/compound 2, and (D) NS5B<sup>GT1a</sup>/HCV-796 versus NS5B<sup>GT1a</sup>/compound 9B. .... 10

52 Figure S7. Distances between BMS-929075 and residues during the last 20 ns MD  
53 trajectories..... 11

54 Figure S8. The tunnels represented by residues Arg394 (skyblue) and Phe551 (warmpink) for  
55 (A) NS5B<sup>GT1a</sup>/BMS-929075 (slate), (B) NS5B<sup>GT1b</sup>/BMS-929075 (salmon), (C)  
56 NS5B<sup>GT2a</sup>/BMS-929075 (yellow orange) and (D) NS5B<sup>GT2b</sup>/BMS-929075 (cyan). .... 12

57 Figure S9. The individual energy term contributions of key residues to the binding free  
58 energies of (A) NS5B<sup>GT1a</sup>/BMS-986139, (B) NS5B<sup>GT1b</sup>/BMS-986139, (C) NS5B<sup>GT2a</sup>/BMS-  
59 986139, and (D) NS5B<sup>GT2b</sup>/BMS-986139 system. .... 13

60 Figure S10. The tunnels represented by residues Arg394 (skyblue) and Phe551 (warmpink)  
61 for (A) NS5B<sup>GT1a</sup>/MK-8876 (cyan), (B) NS5B<sup>GT1b</sup>/MK-8876 (orange), (C) NS5B<sup>GT2a</sup>/MK-  
62 8876 (salmon) and (D) NS5B<sup>GT2b</sup>/MK-8876 (limon)..... 14

63 Figure S11. Distances between MK-8876 and residues during the last 20 ns MD trajectories.  
64 ..... 15

65 Figure S12. The individual energy term contributions of key residues to the binding free  
66 energies of (A) NS5B<sup>GT1a</sup>/MK-8876, (B) NS5B<sup>GT1b</sup>/MK-8876, (C) NS5B<sup>GT2a</sup>/MK-8876, and  
67 (D) NS5B<sup>GT2b</sup>/MK-8876 system. .... 16

68 Figure S13. The tunnels represented by residues Arg394 (skyblue) and Phe551 (warmpink)  
69 for (A) NS5B<sup>GT1a</sup>/compound 2 (green), (B) NS5B<sup>GT1b</sup>/compound 2 (cyan), (C)  
70 NS5B<sup>GT2a</sup>/compound 2 (orange) and (D) NS5B<sup>GT2b</sup>/compound 2 (yellow). .... 17

71 Figure S14. Distances between compound 2 and residues during the last 20 ns MD  
72 trajectories..... 18

73 Figure S15. The individual energy term contributions of key residues to the binding free  
74 energies of (A) NS5B<sup>GT1a</sup>/compound 2, (B) NS5B<sup>GT1b</sup>/compound 2, (C) NS5B<sup>GT2a</sup>/compound  
75 2 and (D) NS5B<sup>GT2b</sup>/compound 2 system. .... 19

76 Figure S16. The tunnels represented by residues Arg394 (skyblue) and Phe551 (warmpink)  
77 for (A) NS5B<sup>GT1a</sup>/compound 9B (orange), (B) NS5B<sup>GT1b</sup>/compound 9B (slate), (C)  
78 NS5B<sup>GT2a</sup>/compound 9B (limon) and (D) NS5B<sup>GT2b</sup>/compound 9B (yellow). .... 20

79 Figure S17. Distances between compound 9B and residues during the last 20 ns MD  
80 trajectories..... 21

81 Figure S18. The individual energy term contributions of key residues to the binding free  
82 energies of (A) NS5B<sup>GT1a</sup>/compound 9B, (B) NS5B<sup>GT1b</sup>/compound 9B, (C)  
83 NS5B<sup>GT2a</sup>/compound 9B and (D) NS5B<sup>GT2b</sup>/compound 9B system. .... 22

84 Summary of Common Residues Contributing to the Binding of Benzofuran Core Inhibitors 23

85 Highlight of Differences in Target Residues or Compound Substituents for Designing More  
86 Efficient or Selective Compounds..... 25

87

88 Table S1. The best docking pose scores and the RMSD values of the docking  
89 structures relative to the crystallographic structures

COMPLEX	Score(kcal/mol)	RMSD	Reference Structure for the RMSD Calculation
NS5B <sup>GT1a</sup> /HCV-796	-10.82	0.264	4KHR
NS5B <sup>GT1a</sup> /BMS-929075	-10.66	0.264	4KHR
NS5B <sup>GT1a</sup> /MK-8876	-11.58	0.264	4KHR
NS5B <sup>GT1a</sup> /compound 2	-12.54	0.264	4KHR
NS5B <sup>GT1a</sup> /compound 9B	-12.53	0.264	4KHR
NS5B <sup>GT1b</sup> /HCV-796	-11.11	0.218	3FQK
NS5B <sup>GT1b</sup> /BMS-929075	-12.48	0.390	5PZP
NS5B <sup>GT1b</sup> /MK-8876	-13.68	0.161	5W2E
NS5B <sup>GT1b</sup> /compound 2	-13.91	0.161	5W2E

NS5B <sup>GT1b</sup> /compound 9B	-14.04	0.161	5W2E
NS5B <sup>GT2a</sup> /HCV-796	-11.51	0.154	5TWM
NS5B <sup>GT2a</sup> /BMS-929075	-12.97	0.154	5TWM
NS5B <sup>GT2a</sup> /MK-8876	-13.98	0.154	5TWM
NS5B <sup>GT2a</sup> /compound 2	-14.41	0.154	5TWM
NS5B <sup>GT2a</sup> /compound 9B	-14.76	0.154	5TWM
NS5B <sup>GT2b</sup> /HCV-796	-11.05	0.160	3GSZ
NS5B <sup>GT2b</sup> /BMS-929075	-11.13	0.160	3GSZ
NS5B <sup>GT2b</sup> /MK-8876	-12.10	0.160	3GSZ
NS5B <sup>GT2b</sup> /compound 2	-12.45	0.160	3GSZ
NS5B <sup>GT2b</sup> /compound 9B	-12.36	0.160	3GSZ

90

91

92

93

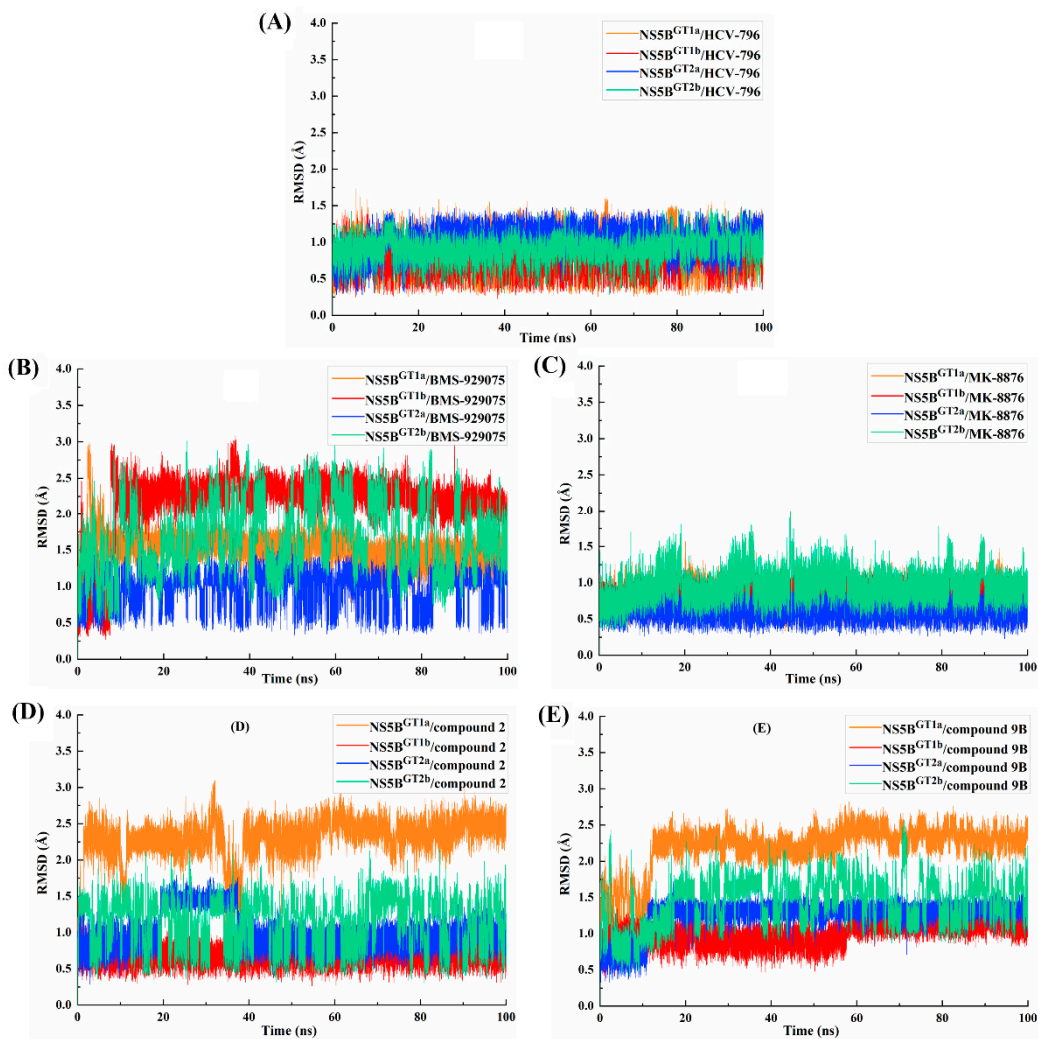
94

95

96

97

98



99

100 Figure S1. The root-mean-square deviations (RMSD) of the ligands in the 20 complex  
 101 systems.

102

103

104

105

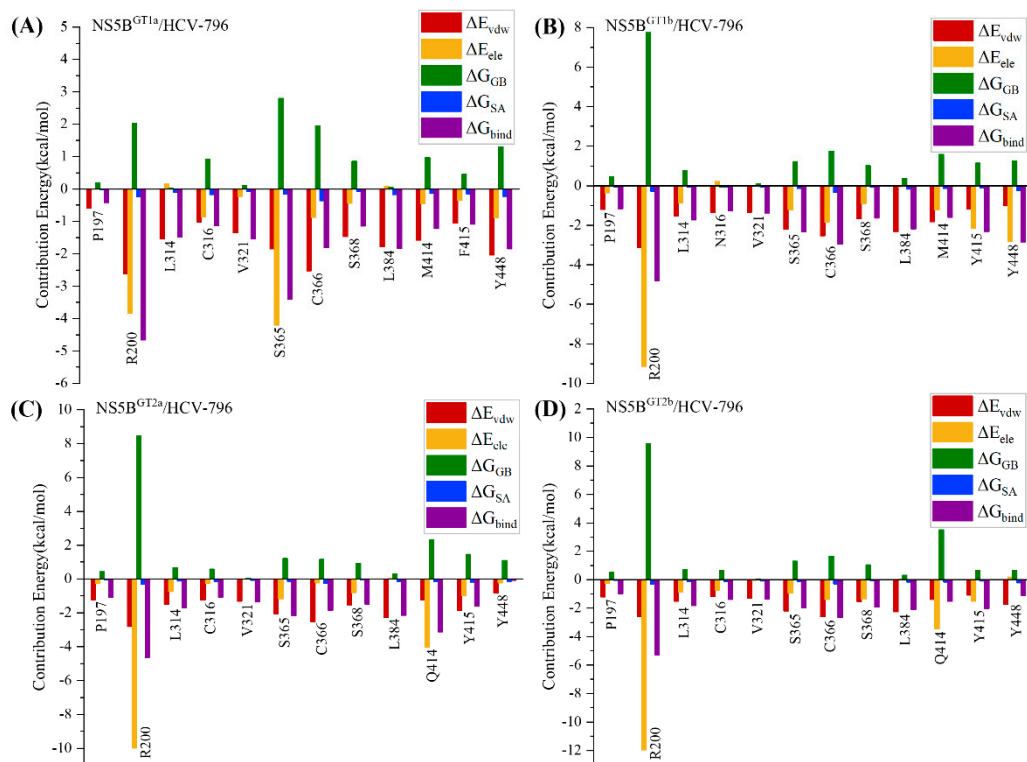
106

107

108

109

110



111

112 Figure S2. The individual energy term contributions of key residues to the binding  
 113 free energies of (A) NS5B<sup>GT1a</sup>/HCV-796, (B) NS5B<sup>GT1b</sup>/HCV-796, (C)  
 114 NS5B<sup>GT2a</sup>/HCV-796, and (D) NS5B<sup>GT2b</sup>/HCV-796 systems.

115

116

117

118

119

120

121

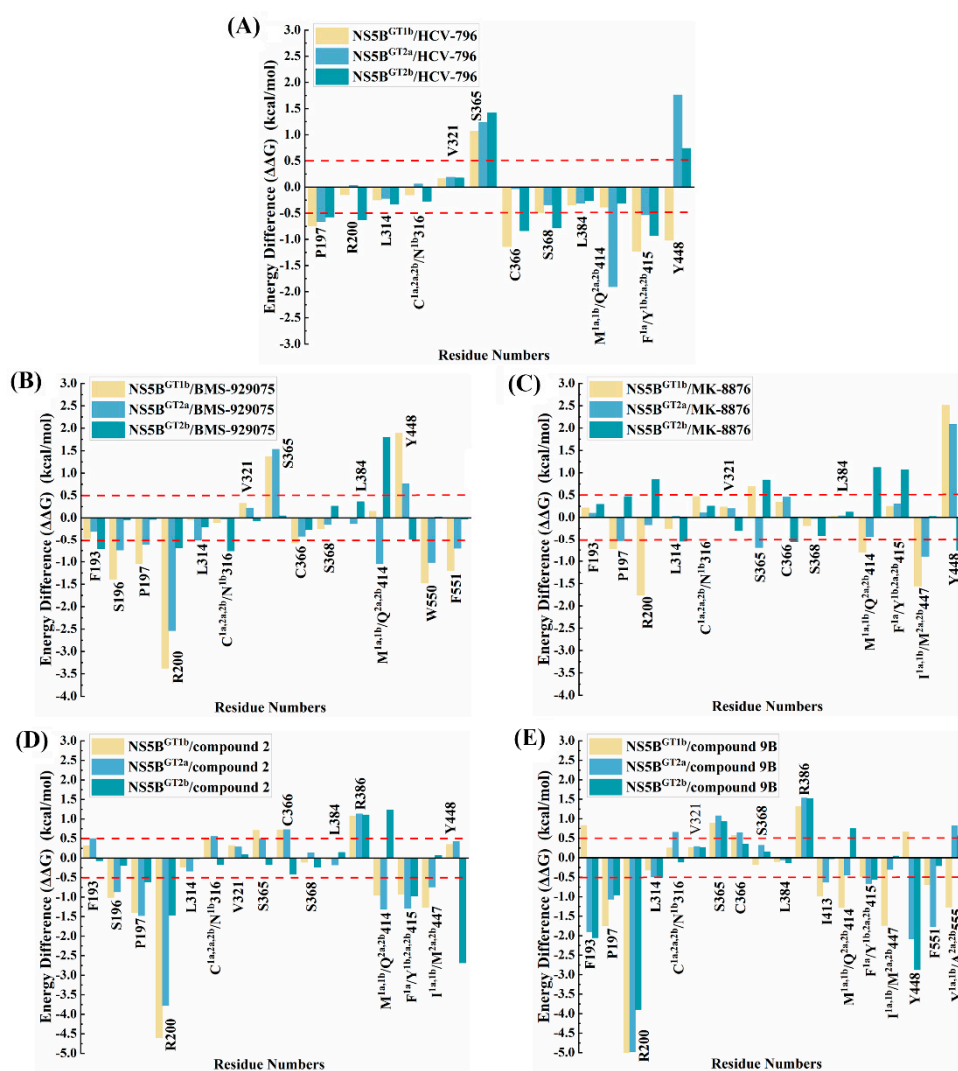
122

123

124

125

126



127

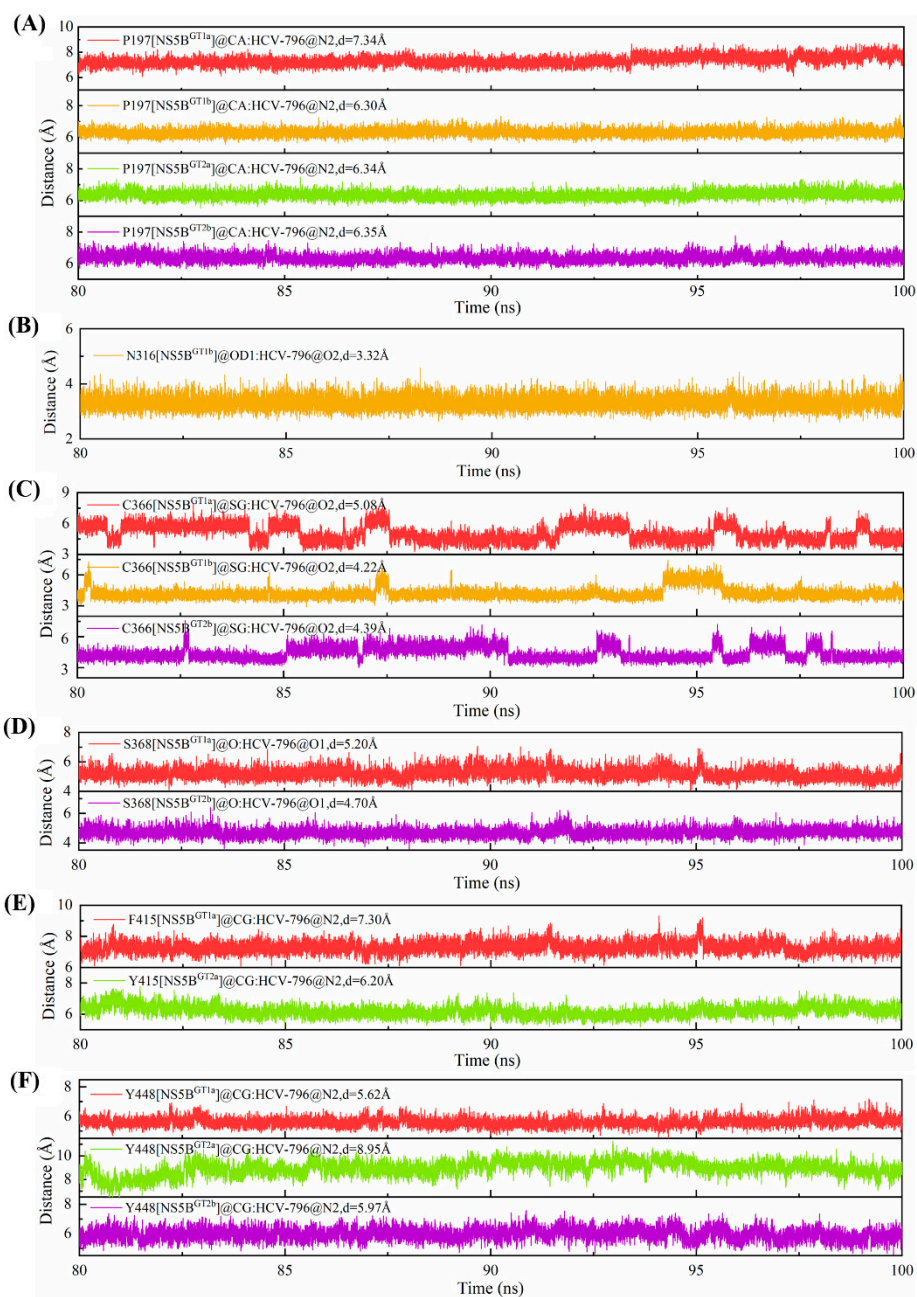
128 Figure S3. The energetic difference ( $\Delta\Delta G = \Delta G_{NS5B^{GT1b/GT2a/GT2b}/inhibitor} -$   
 129  $\Delta G_{NS5B^{GT1a}/inhibitor}$ ) spectra of the corresponding key residues between the  
 130  $NS5B^{GT1a}$  system and the  $NS5B^{GT1b}$  system,  $NS5B^{GT2a}$  system, or  $NS5B^{GT2b}$  system.  
 131 (A)  $NS5B/HCV-796$ ; (B)  $NS5B/BMS-929075$ ; (C)  $NS5B/MK-8876$ ; (D)  
 132  $NS5B/compound\ 2$ ; (E)  $NS5B/compound\ 9B$ .

133

134

135

136



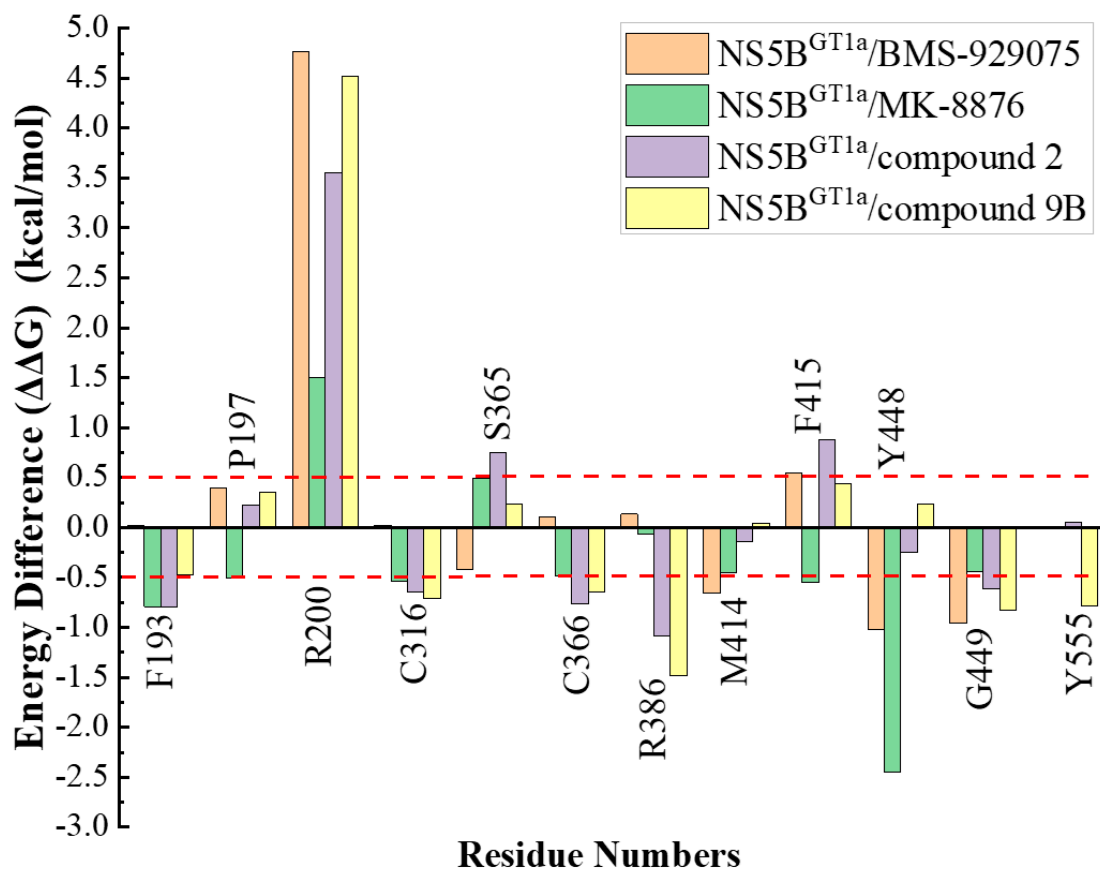
137

138 Figure S4. Distances between HCV-796 and residues during the last 20 ns MD  
 139 trajectories.

140

141

142



143

144 Figure S5. The energetic difference spectra between the NS5B<sup>GT1a</sup>/HCV-796 system  
 145 and the NS5B<sup>GT1a</sup>/BMS-929075, NS5B<sup>GT1a</sup>/MK-8876, NS5B<sup>GT1a</sup>/compound 2 or  
 146 NS5B<sup>GT1a</sup>/compound 9B system ( $\Delta\Delta G = \Delta G_{NS5B^{GT1a}/(BMS-929075/MK-}$   
 147  $8876/compound\ 2/compound\ 9B)} - \Delta G_{NS5B^{GT1a}/HCV-796}$ ).

148

149

150

151

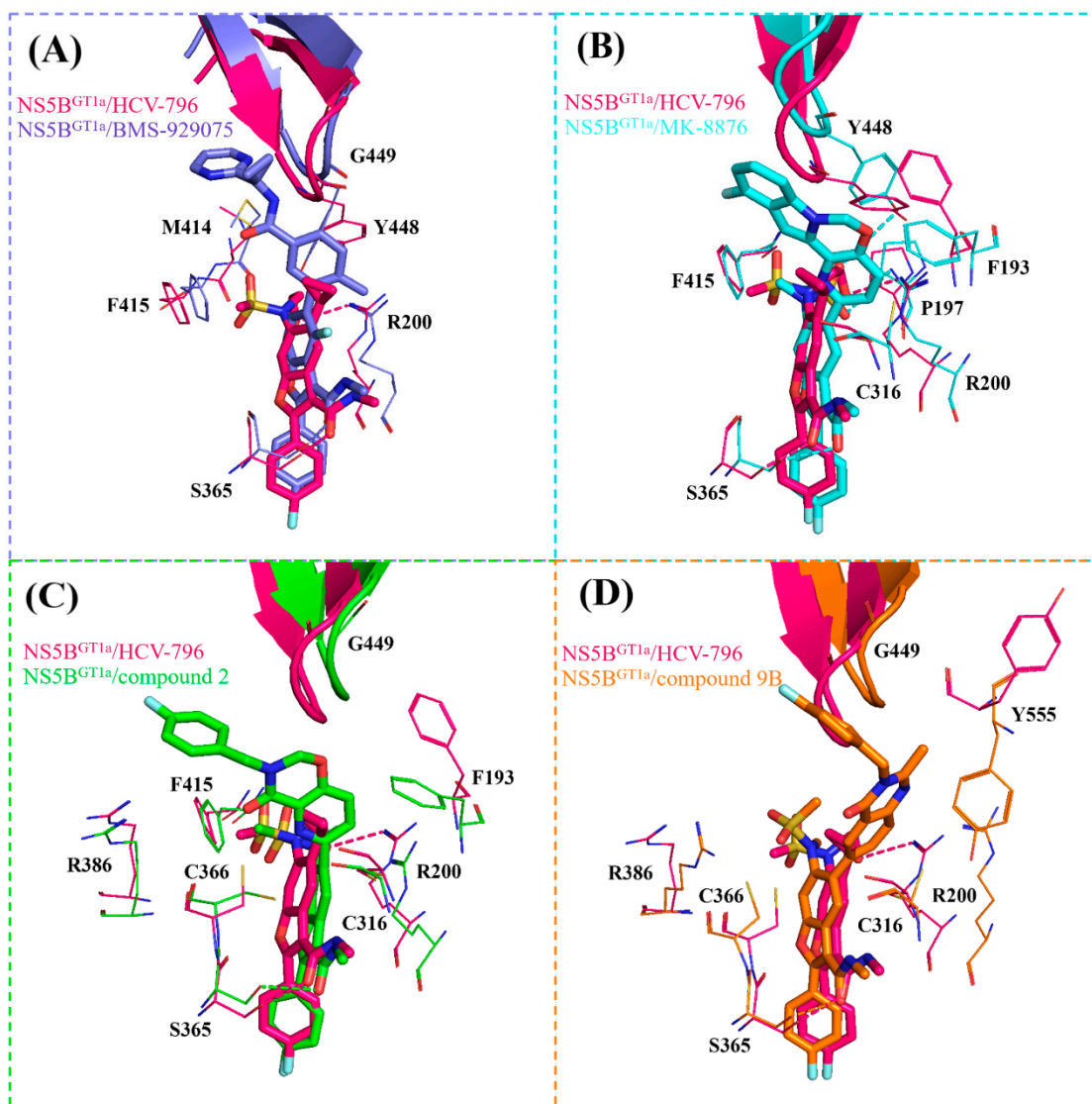
152

153

154

155

156



157

158 Figure S6. The binding modes of (A) NS5B<sup>GT1a</sup>/HCV-796 versus NS5B<sup>GT1a</sup>/BMS-  
 159 929075, (B) NS5B<sup>GT1a</sup>/HCV-796 versus NS5B<sup>GT1a</sup>/MK-8876, (C) NS5B<sup>GT1a</sup>/HCV-  
 160 796 versus NS5B<sup>GT1a</sup>/compound 2, and (D) NS5B<sup>GT1a</sup>/HCV-796 versus  
 161 NS5B<sup>GT1a</sup>/compound 9B.

162

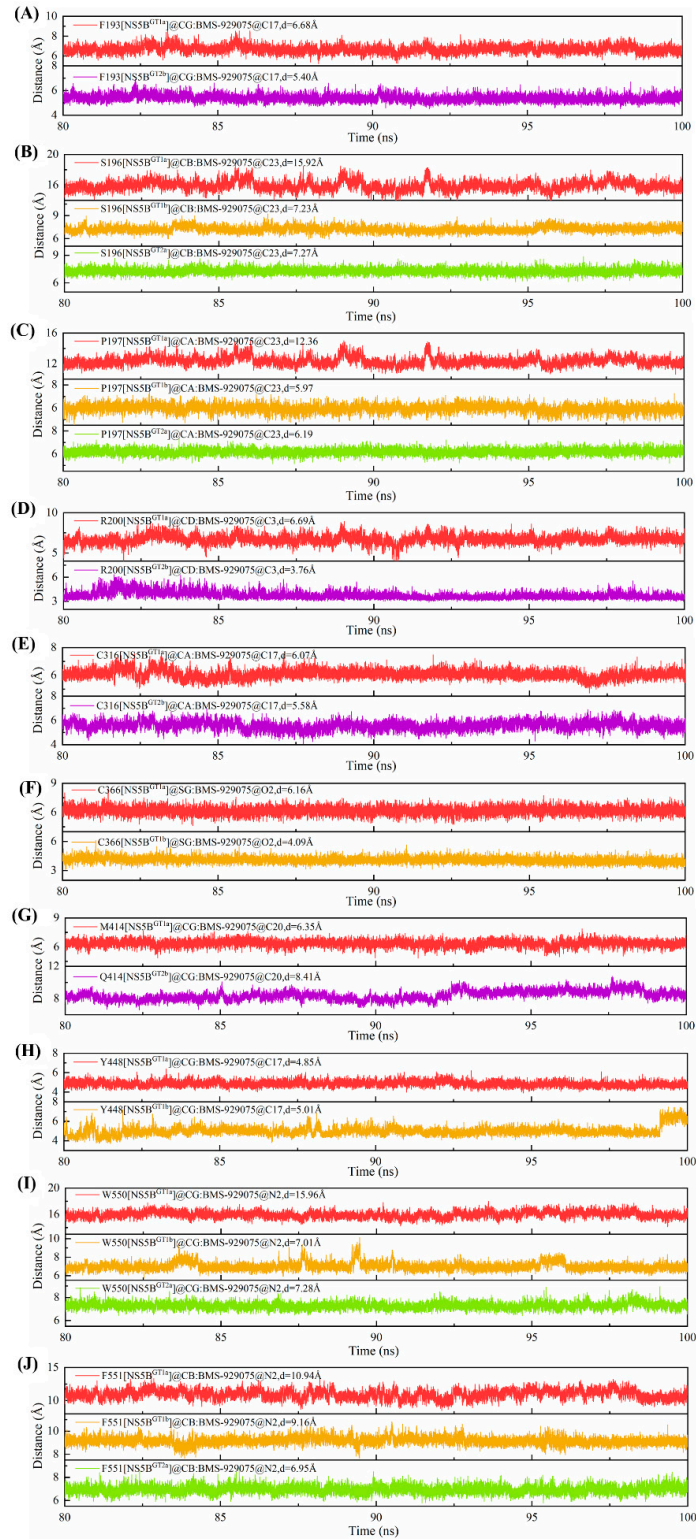
163

164

165

166

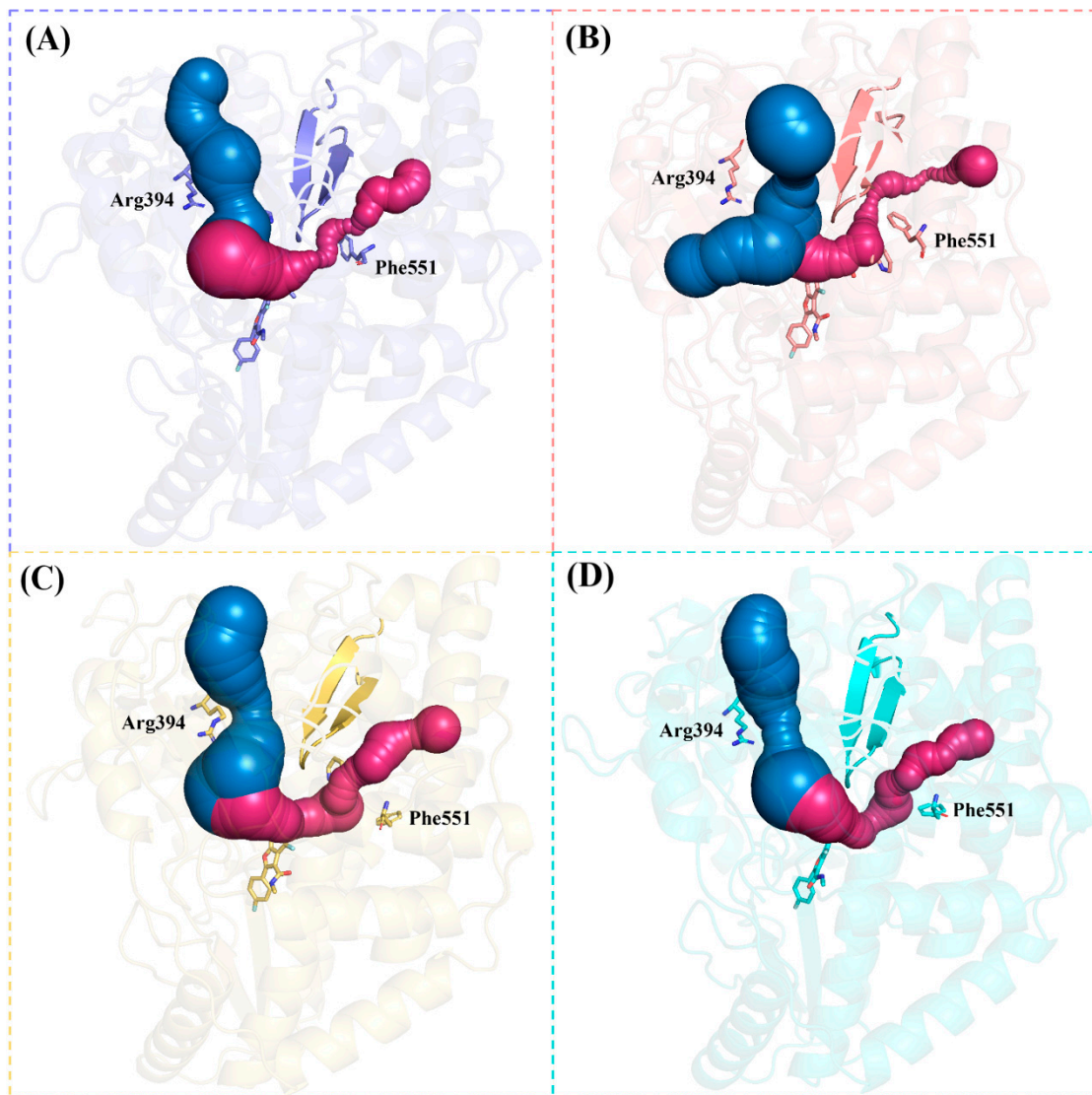
167



168

169 Figure S7. Distances between BMS-929075 and residues during the last 20 ns MD  
 170 trajectories.

171



172

173 Figure S8. The tunnels represented by residues Arg394 (skyblue) and Phe551  
 174 (warmpink) for (A) NS5B<sup>GT1a</sup>/BMS-929075 (slate), (B) NS5B<sup>GT1b</sup>/BMS-929075  
 175 (salmon), (C) NS5B<sup>GT2a</sup>/BMS-929075 (yellow orange) and (D) NS5B<sup>GT2b</sup>/BMS-  
 176 929075 (cyan).

177

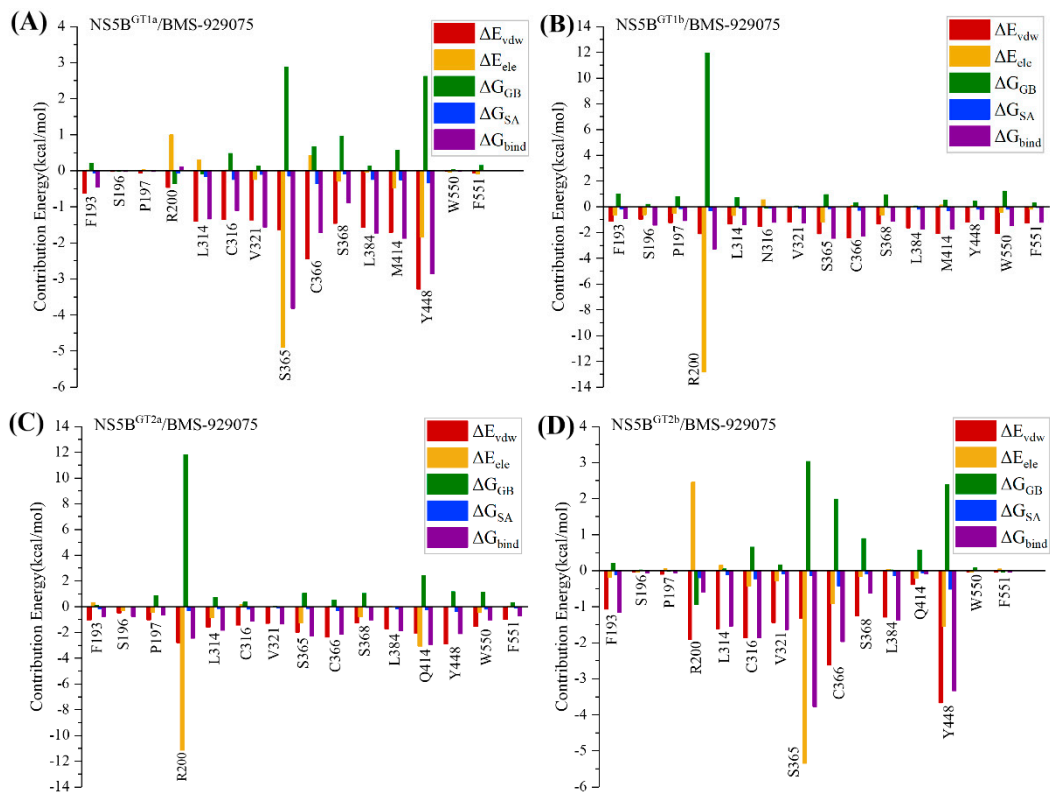
178

179

180

181

182



183

184 Figure S9. The individual energy term contributions of key residues to the binding  
 185 free energies of (A) NS5B<sup>GT1a</sup>/BMS-986139, (B) NS5B<sup>GT1b</sup>/BMS-986139, (C)  
 186 NS5B<sup>GT2a</sup>/BMS-986139, and (D) NS5B<sup>GT2b</sup>/BMS-986139 system.

187

188

189

190

191

192

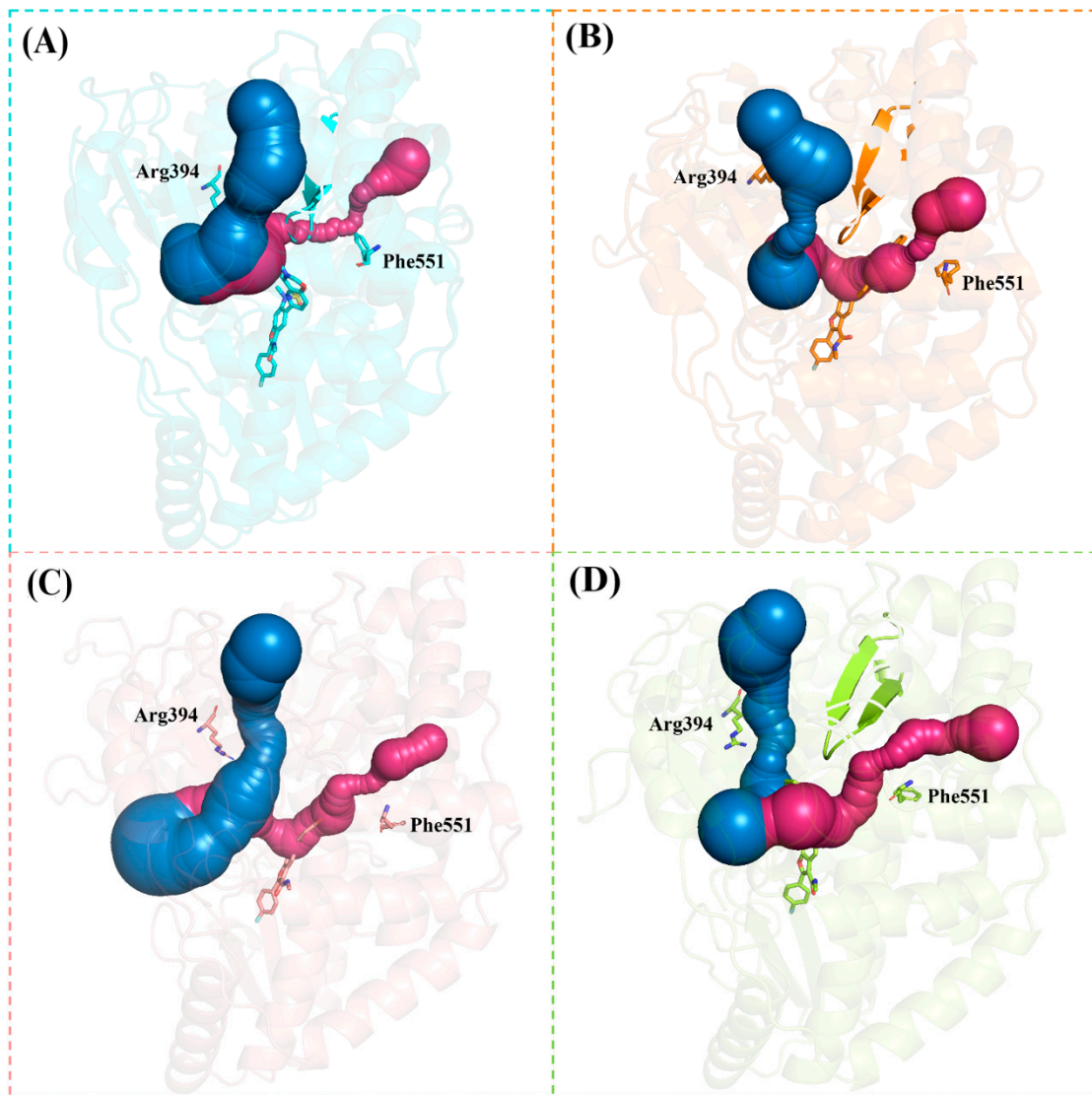
193

194

195

196

197



198

199 Figure S10. The tunnels represented by residues Arg394 (skyblue) and Phe551  
 200 (warmpink) for (A) NS5B<sup>GT1a</sup>/MK-8876 (cyan), (B) NS5B<sup>GT1b</sup>/MK-8876 (orange),  
 201 (C) NS5B<sup>GT2a</sup>/MK-8876 (salmon) and (D) NS5B<sup>GT2b</sup>/MK-8876 (limon).

202

203

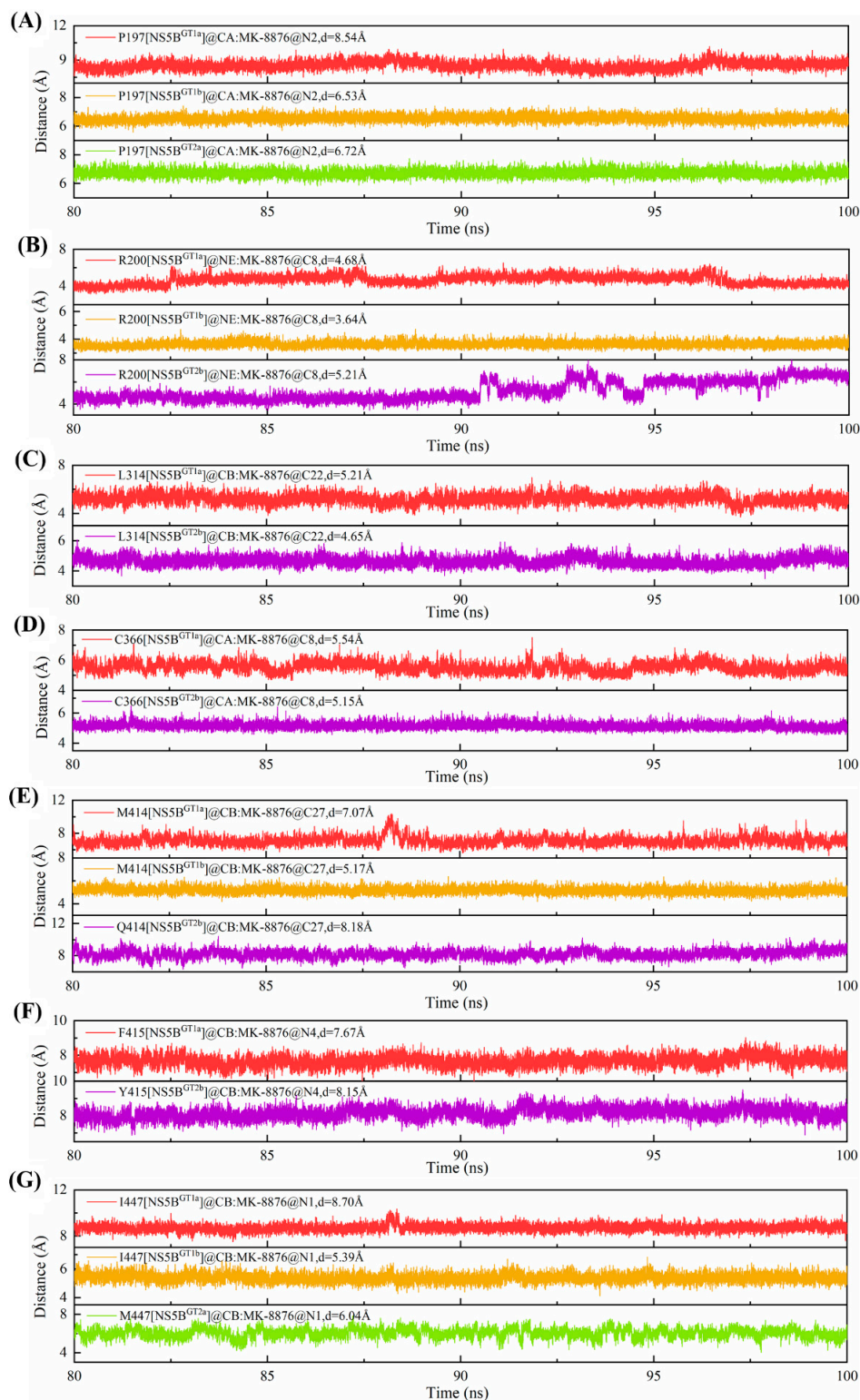
204

205

206

207

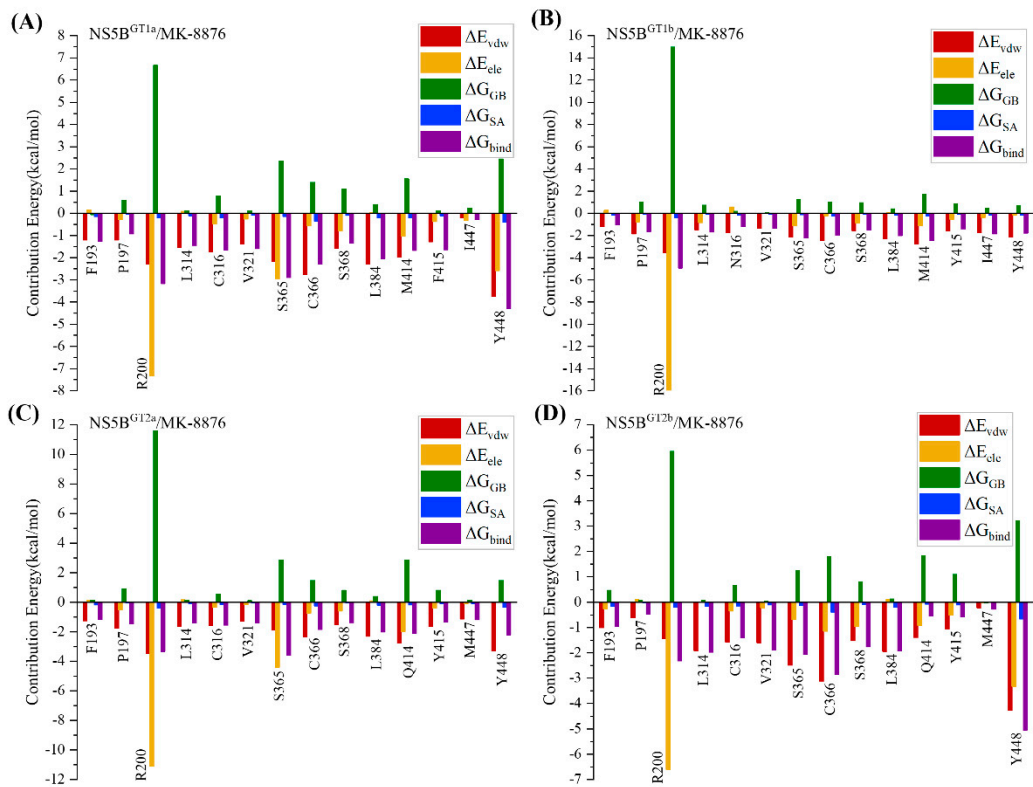
208



209

210 Figure S11. Distances between MK-8876 and residues during the last 20 ns MD  
 211 trajectories.

212



213

214 Figure S12. The individual energy term contributions of key residues to the binding  
 215 free energies of (A) NS5B<sup>GT1a</sup>/MK-8876, (B) NS5B<sup>GT1b</sup>/MK-8876, (C)  
 216 NS5B<sup>GT2a</sup>/MK-8876, and (D) NS5B<sup>GT2b</sup>/MK-8876 system.

217

218

219

220

221

222

223

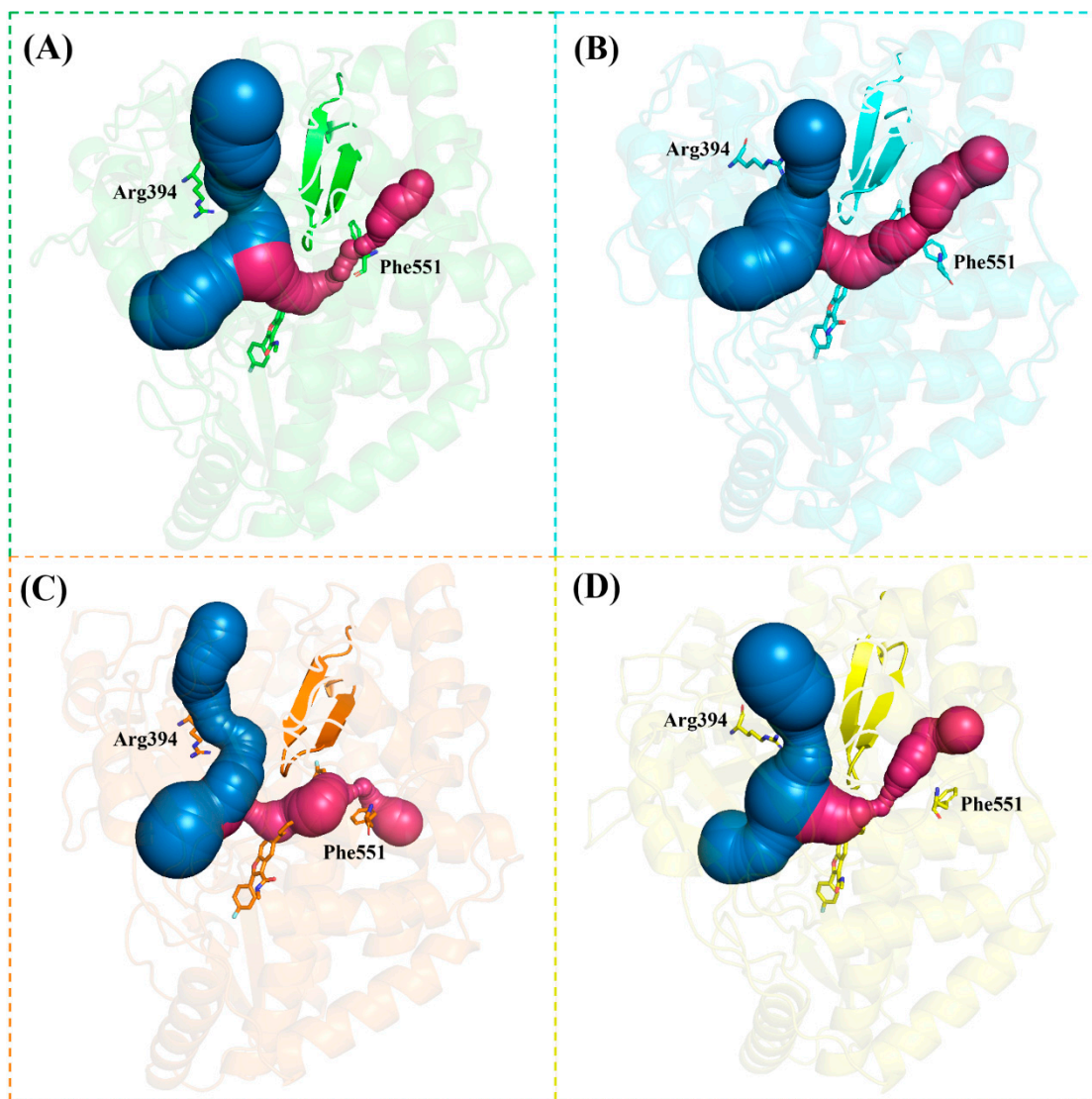
224

225

226

227

228



229

230 Figure S13. The tunnels represented by residues Arg394 (skyblue) and Phe551  
 231 (warmpink) for (A) NS5B<sup>GT1a</sup>/compound 2 (green), (B) NS5B<sup>GT1b</sup>/compound 2  
 232 (cyan), (C) NS5B<sup>GT2a</sup>/compound 2 (orange) and (D) NS5B<sup>GT2b</sup>/compound 2 (yellow).

233

234

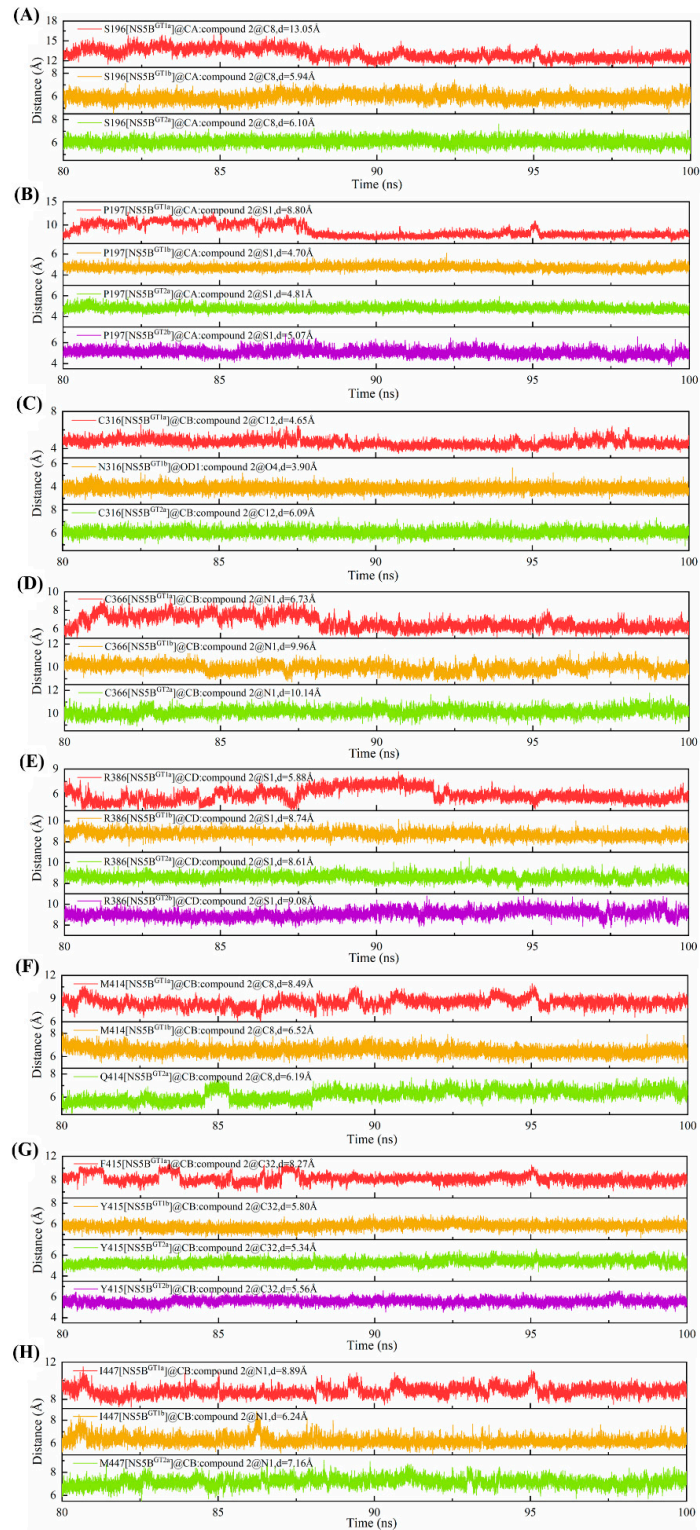
235

236

237

238

239



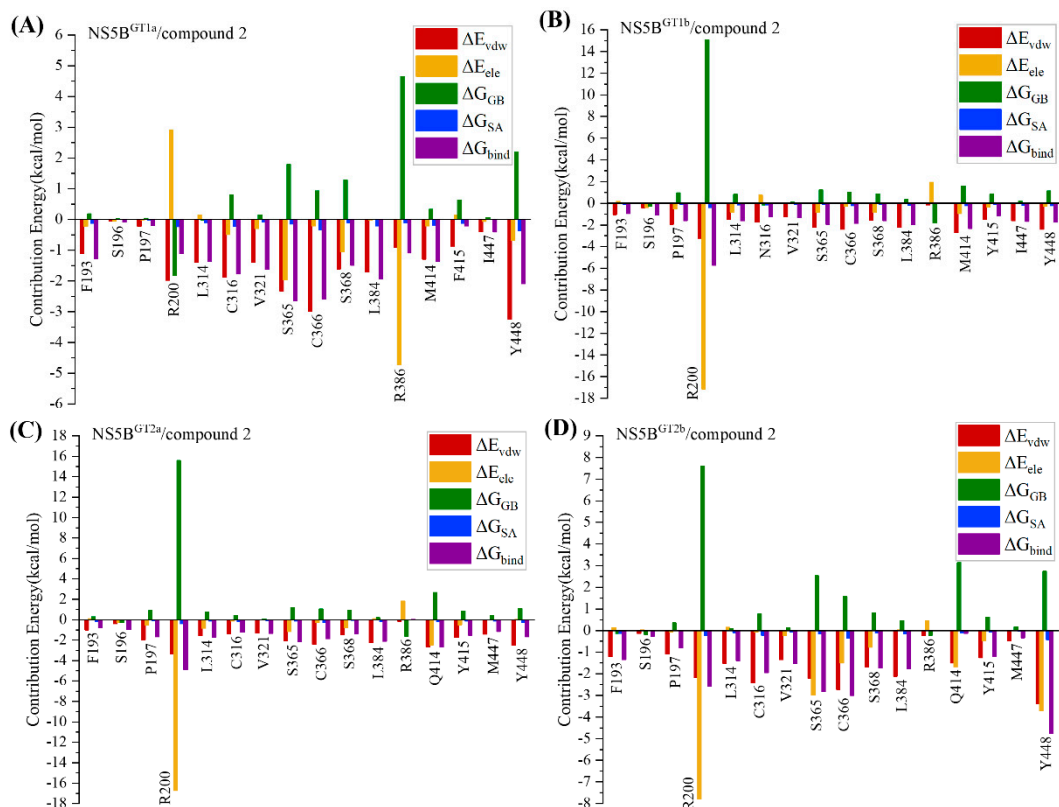
240

241 Figure S14. Distances between compound 2 and residues during the last 20 ns MD

242

trajectories.

243



244

245 Figure S15. The individual energy term contributions of key residues to the binding  
 246 free energies of (A) NS5B<sup>GT1a</sup>/compound 2, (B) NS5B<sup>GT1b</sup>/compound 2, (C)  
 247 NS5B<sup>GT2a</sup>/compound 2 and (D) NS5B<sup>GT2b</sup>/compound 2 system.

248

249

250

251

252

253

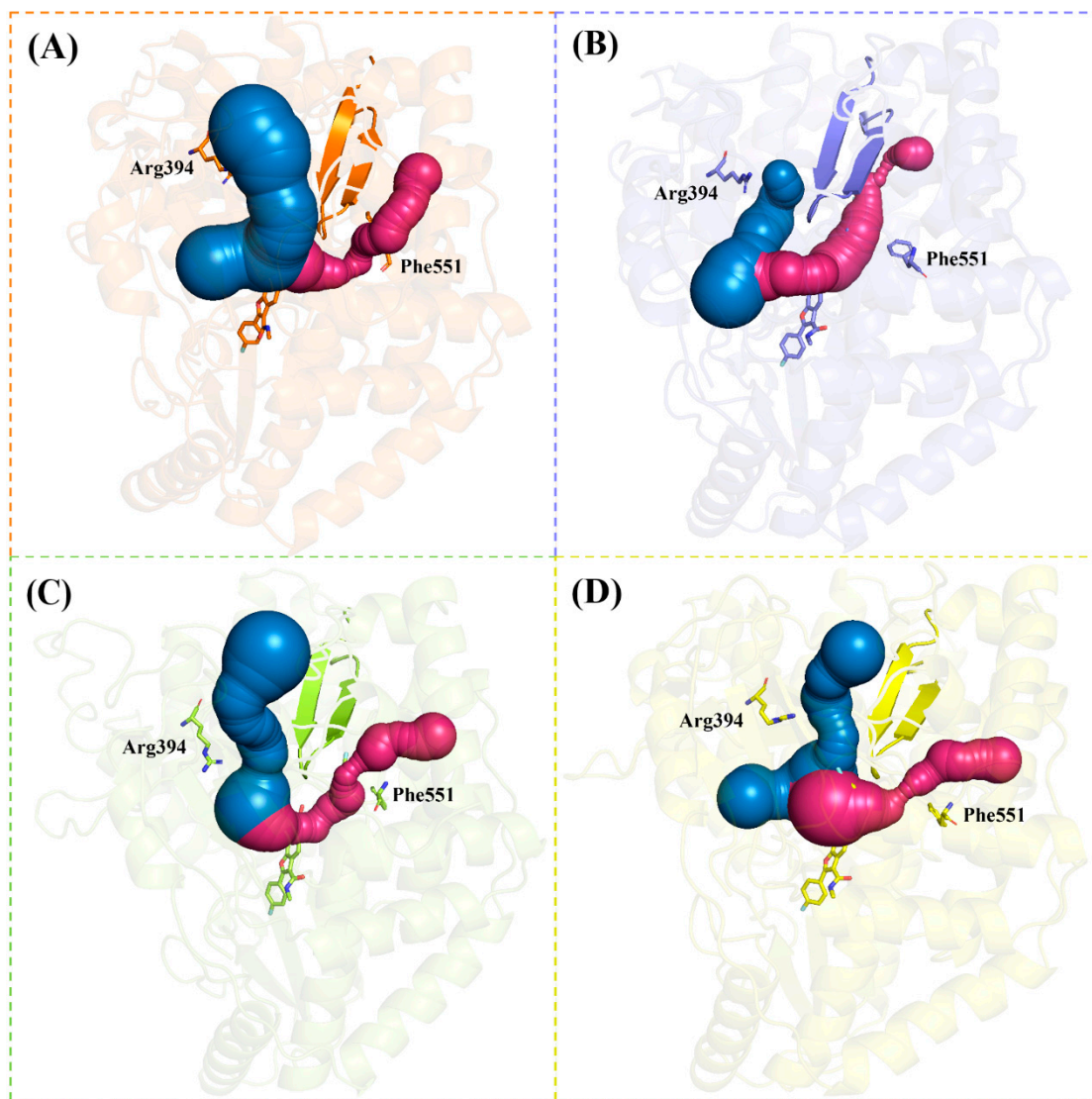
254

255

256

257

258

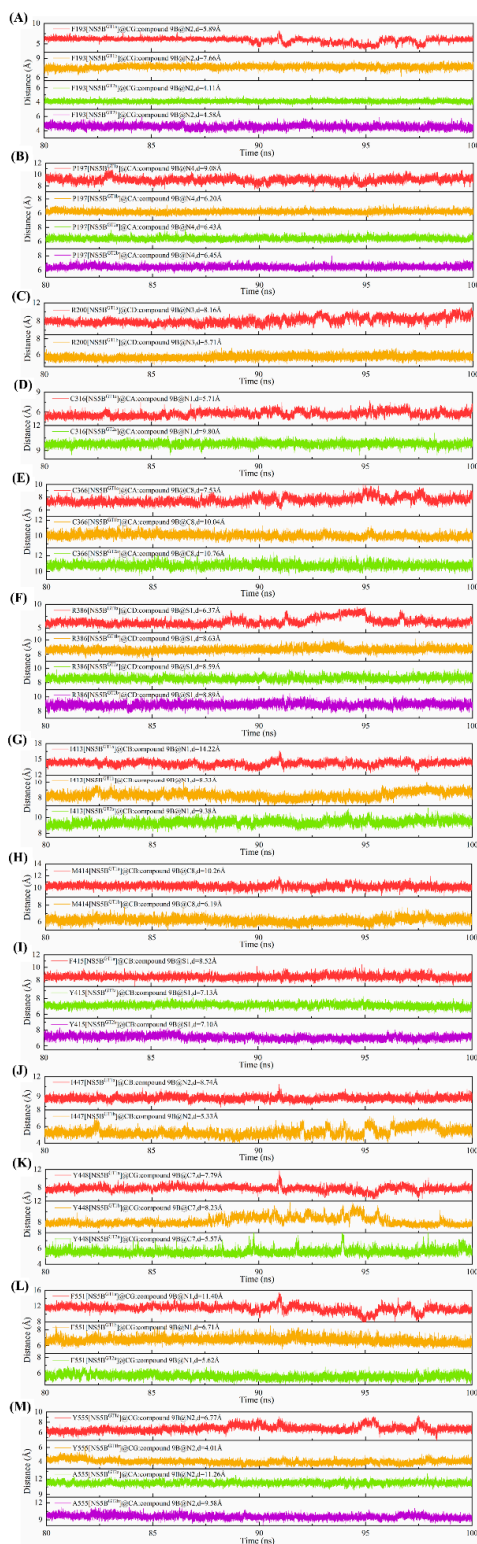


259

260 Figure S16. The tunnels represented by residues Arg394 (skyblue) and Phe551  
 261 (warmpink) for (A) NS5B<sup>GT1a</sup>/compound 9B (orange), (B) NS5B<sup>GT1b</sup>/compound 9B  
 262 (slate), (C) NS5B<sup>GT2a</sup>/compound 9B (limon) and (D) NS5B<sup>GT2b</sup>/compound 9B  
 263 (yellow).

264

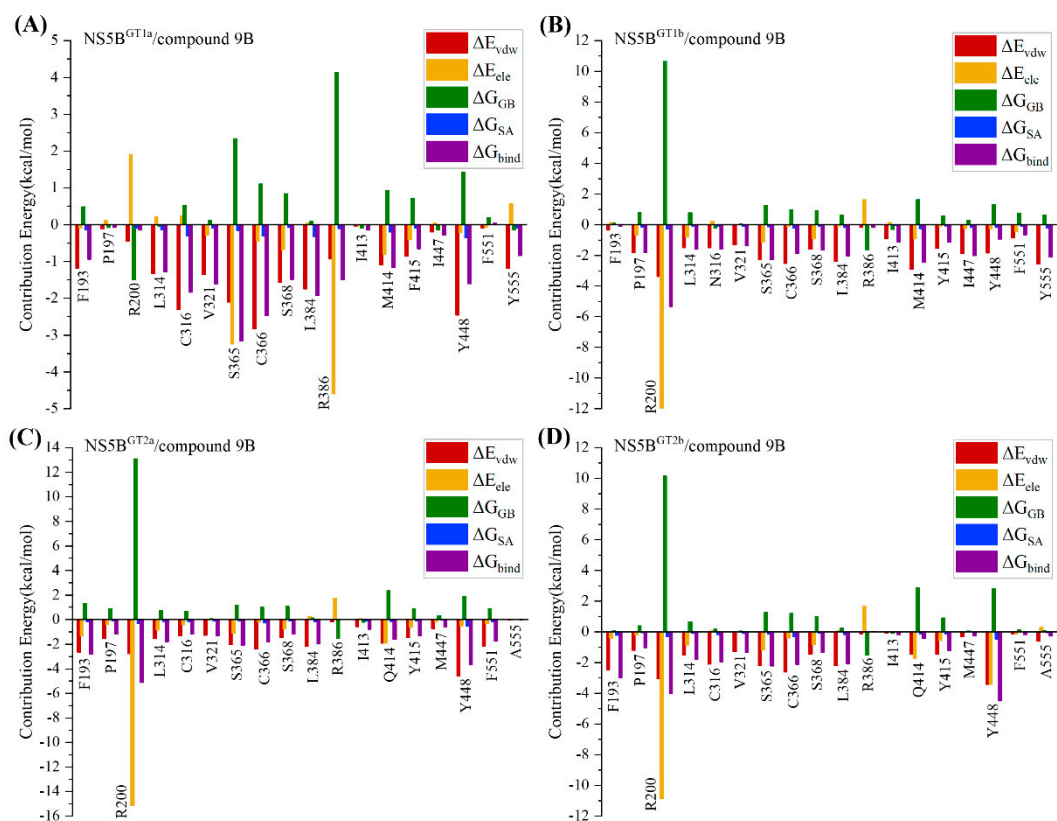
265



266

267 Figure S17. Distances between compound 9B and residues during the last 20 ns MD  
 268 trajectories.

269



270

271 Figure S18. The individual energy term contributions of key residues to the binding  
 272 free energies of (A) NS5B<sup>GT1a</sup>/compound 9B, (B) NS5B<sup>GT1b</sup>/compound 9B,  
 273 NS5B<sup>GT2a</sup>/compound 9B and (D) NS5B<sup>GT2b</sup>/compound 9B system.

274

275

276

277

278

279

280

281

282

283

284

285

286

287

288 **Summary of Common Residues Contributing to the Binding of Benzofuran Core**  
289 **Inhibitors**

290 The benzofuran core inhibitors, including HCV-796, BMS-929075, MK-8876,  
291 compound 2, and compound 9B, exhibit significant pan-genotypic activity against  
292 various genotypes of the NS5B polymerase of the hepatitis C virus (HCV). Molecular  
293 simulations, including molecular docking, molecular dynamics (MD) simulations,  
294 MM/GBSA energy calculations, and adaptive steered molecular dynamics (ASMD)  
295 simulations, were used to elucidate their binding mechanisms. The results highlight  
296 several common residues that play crucial roles in the binding of these inhibitors to the  
297 NS5B polymerase across different genotypes (GT1a, 1b, 2a, and 2b). These key  
298 residues are predominantly located within the Palm II subdomain and its overlapping  
299 regions with Palm I and Palm III subdomains of the NS5B polymerase.

300 **Key Residues and Their Contributions**

301 1. Arg200: This residue is involved in significant interactions with all five  
302 inhibitors. It frequently forms hydrogen bonds and contributes to the electrostatic  
303 interactions, playing a critical role in stabilizing the inhibitor binding.

304 2. Leu314: Contributes mainly through van der Waals interactions, providing  
305 hydrophobic stability to the inhibitor binding.

306 3. Cys316/Asn316: Depending on the genotype, this residue contributes through  
307 hydrogen bonding and van der Waals interactions. Notably, Asn316 in GT1b forms  
308 additional hydrogen bonds due to its polar side chain.

309 4. Val321: Engages in hydrophobic interactions with the inhibitors, contributing  
310 to van der Waals forces that stabilize the binding.

311 5. Ser365: Frequently forms hydrogen bonds with the inhibitors, particularly with  
312 HCV-796 and MK-8876, indicating its importance in polar interactions.

313 6. Cys366: Contributes through both van der Waals and electrostatic interactions,  
314 enhancing the overall binding strength of the inhibitors.

315 7. Ser368: Forms hydrogen bonds with some inhibitors and contributes to the  
316 binding through polar interactions.

317 8. Leu384: Involved in hydrophobic interactions, contributing to the stability of  
318 the inhibitor binding through van der Waals forces.

319 9. Met414/Gln414: Depending on the genotype, this residue participates in  
320 hydrophobic and polar interactions, significantly affecting binding affinity.

321 10. Phe415/Tyr415: These residues engage in hydrophobic interactions and, in the  
322 case of Tyr415 in GT1b, additional hydrogen bonding, significantly enhancing binding  
323 strength.

324 11. Tyr448: Consistently forms hydrogen bonds with various inhibitors,  
325 contributing to both polar and hydrophobic interactions.

### 326 **Binding Modes and Interaction Patterns**

327 The binding of benzofuran core inhibitors is characterized by extensive interactions  
328 with residues in the Palm II subdomain and its overlapping regions with Palm I and  
329 Palm III subdomains. The interactions include hydrogen bonds, van der Waals forces,  
330 and electrostatic contributions. The van der Waals interactions, particularly with  
331 residues such as Leu314, Val321, and Leu384, are crucial for the stable binding of the  
332 inhibitors. Polar residues like Arg200, Ser365, and Tyr448 often form hydrogen bonds,  
333 further stabilizing the inhibitor-NS5B complex.

334 The detailed binding modes and interaction patterns elucidated by the simulations  
335 provide valuable insights for the design and optimization of novel benzofuran core  
336 inhibitors with enhanced pan-genotypic activity against HCV NS5B polymerase.

337

338

339

340

341

342

343

344

345

346

347 **Highlight of Differences in Target Residues or Compound Substituents for**  
348 **Designing More Efficient or Selective Compounds**

349 The study on benzofuran core inhibitors reveals significant differences in target  
350 residues and compound substituents that could be leveraged to design more efficient  
351 and selective inhibitors against various genotypes of the NS5B polymerase. The key  
352 findings from the binding mode analyses and molecular simulations highlight several  
353 critical aspects:

354 **Differences in Target Residues**

355 1. **Cys316 vs. Asn316 (GT1a vs. GT1b):**

356 **Cys316 (GT1a):** Primarily involved in van der Waals interactions.

357 **Asn316 (GT1b):** Engages in additional hydrogen bonding due to its polar side  
358 chain, enhancing binding strength.

359 2. **Phe415 vs. Tyr415 (GT1a vs. GT1b/GT2a/GT2b):**

360 **Phe415 (GT1a):** Contributes mainly through hydrophobic interactions.

361 **Tyr415 (GT1b/GT2a/GT2b):** Forms stronger hydrogen bonds with inhibitors,  
362 significantly enhancing binding affinity.

363 3. **Met414 vs. Gln414 (GT1a/GT1b vs. GT2a/GT2b):**

364 **Met414 (GT1a/GT1b):** Participates in hydrophobic interactions.

365 **Gln414 (GT2a/GT2b):** Involved in polar interactions, contributing to a  
366 different binding dynamic.

367 4. **Tyr448:**

368 **GT2b:** Forms stronger hydrogen bonds compared to other genotypes,  
369 suggesting genotype-specific interactions that could be targeted for selective  
370 inhibition.

371 **Differences in Compound Substituents**

372 1. **C5 Position Substituents:**

373 **Longer Substituents (e.g., BMS-929075, MK-8876, compound 2, compound**  
374 **9B):** Exhibit different binding patterns between GT1a/2b and GT1b/2a,  
375 indicating that modifications at the C5 position can be tailored to enhance

376 selectivity and potency across different genotypes.

## 377 2. **Para-Fluorophenyl Groups at C2 Position:**

378 **Interaction Variations:** The para-fluorophenyl groups at the C2 position  
379 interact differently with residues across various genotypes, suggesting that  
380 modifying this substituent could optimize binding affinity and specificity.

### 381 **Design Implications**

382 • **Targeting Polar Residues:** Enhancing interactions with polar residues like  
383 Asn316 and Gln414 can improve binding strength in genotypes where these  
384 residues are present, such as GT1b and GT2b.

385 • **Substituent Optimization:** Modifying the substituents at the C5 and C2  
386 positions to enhance specific interactions with key residues like Tyr415 and  
387 Tyr448 can lead to more selective inhibitors.

388 • **Hydrophobic vs. Polar Balancing:** Balancing hydrophobic and polar  
389 interactions by adjusting substituents can optimize binding across different  
390 genotypes, as seen with the varied contributions of residues like Cys316 and  
391 Asn316.

### 392 **Example Binding Modes**

393 • **HCV-796:** Forms multiple hydrogen bonds and hydrophobic interactions, but  
394 its hepatotoxicity suggests the need for substituent modifications to reduce off-  
395 target effects.

396 • **BMS-929075 and MK-8876:** Show strong binding across multiple genotypes,  
397 indicating that their structural features, such as longer C5 substituents, are  
398 beneficial for pan-genotypic activity.

399 These insights provide a foundation for designing novel benzofuran core inhibitors  
400 with improved efficiency and selectivity by focusing on the differences in target  
401 residues and optimizing compound substituents accordingly.

402  
403